J. Membrane Biol. 92, 183–193 (1986)

The Journal of
Membrane Biology

Osmotic Water Permeabilities of Brush Border and Basolateral Membrane Vesicles from Rat Renal Cortex and Small Intestine

M.P.E. van Heeswijk and C.H. van Os
Department of Physiology, University of Nijmegen, 6500 HB Nijmegen, The Netherlands

Summary. The osmotic water permeability P_f of brush border (BBM) and basolateral (BLM) membrane vesicles from rat small intestine and renal cortex was studied by means of stopped-flow spectrophotometry. Scattered light intensity was used to follow vesicular volume changes upon osmotic perturbation with hypertonic mannitol solutions. A theoretical analysis of the relationship of scattered light intensity and vesicular volume justified a simple exponential approximation of the change in scattered light intensity. The rate constants extracted from fits to an exponential function were proportional to the final medium osmolarity as predicted by theory. For intestinal membranes, computer analysis of optical responses fitted well with a single-exponential treatment. For renal membranes a double-exponential treatment was needed, implying two distinct vesicle populations. P_f values for BBM and BLM preparations of small intestine were equal and amount to 60 μm/sec. For renal preparations, P_f values amount to 600 μm/sec for the fast component, BBM as well as BLM, and to 50 (BBM) and 99 (BLM) μm/sec for the slow component. The apparent activation energy for water permeation in intestinal membranes was 13.3 ± 0.6 and in renal membranes 1.0 ± 0.3 kCal/mole, between 25 and 35°C. The mercurial sulfhydryl reagent *p*CMBS inhibited completely and reversibly the high P_f value in renal brush border preparations. These observations suggest that in intestinal membranes water moves through the lipid matrix but that in renal plasma membranes water channels may be involved. From the high P_f values of renal membrane vesicles a transcellular water permeability for proximal tubules can be calculated which amounts to ~1 cm/sec. This value allows for an entirely transcellular route for water flow during volume reabsorption.

Key Words osmotic water permeability · proximal tubule · epithelial membrane vesicles · brush border membrane · small intestine · basolateral membrane

Introduction

The interpretation of observed transepithelial water permeability data of intact tissue is controversial and there has been considerable debate over the meaning and the magnitude of P_f values [2, 6, 18]. Pitfalls in studying water flows across intact epithelia are unstirred layers, time resolution of flow measurements, membrane area amplification and the route of water flow, cellular *vs.* paracellular. These problems can be circumvented when osmotic flows are measured across isolated membrane vesicles with a stopped-flow technique in which scattered light intensity is used to follow vesicular volume changes. The advantage is that volume flows are monitored continuously with time resolution of 2 to 3 msec and osmotic flows are related to real membrane area without interference of unstirred layers. The disadvantage is that vesicle populations may be inhomogeneous in size and composition. The technique has been widely used to determine solute and water permeabilities [1, 19, 25, 28, 32, 35, 36, 42]. In the present study we used brush border as well as basolateral membrane preparations from small intestine and renal cortex in an attempt to determine the physiological relevance of osmotic measurements on isolated membrane preparations. The theoretical aspects have been considered and tested experimentally. Obtained P_f values were discussed in view of recent measurements on intact cells with a combination of Nomarski optics and a computerized video technique [4, 30, 39].

Materials and Methods

Membrane Preparations

Brush border membranes of rat small intestine were isolated according to the Mg^{2+} precipitation method described by Hauser et al. [13]. Rat renal brush border membranes were isolated with two subsequent Mg^{2+} precipitation steps according to Biber et al. [3]. Basolateral membranes of rat small intestine were isolated as before [11]. Rat kidney cortex basolateral membranes were isolated by means of centrifugation in 38% sucrose followed by centrifugation in 8% Percoll® [15]. All membrane vesicle preparations were washed in 100 mM mannitol, 2 mM $MgCl_2$ and 5 mM HEPES/Tris, pH 7.4, spun down at 100,000 × *g* for 20 min and resuspended in the same medium. The membrane preparations

were used for experiments either freshly or after storage in liquid N_2 within 5 days. No difference in P_f values between membrane vesicles freshly used or after storage was noticed. Enzymes and protein were assayed as previously [11, 15]. Purification factors for the relevant marker enzymes were as given in the original publication.

Stopped-Flow Experiments and Light-Scatter Measurements

Light-scatter intensity was measured using an Aminco Morrow stopped-flow apparatus mounted on an Aminco DW2a spectrophotometer. The photomultiplier tube was mounted on the stopped-flow unit under 90° with the incedent beam from the DW2a monochromator. The photomultiplier signal was amplified with an Aminco photomultiplier microphotometer and this amplified signal was visualized on the monitor of an Apple IIe computer and stored with an appropriate time base.

To perform the experiments, 50 to 200 μl of a concentrated vesicle suspension was diluted into 2.7 ml 100 mM mannitol, 2 mM $MgCl_2$ and 5 mM HEPES/Tris, pH 7.4. One of the syringes of the stopped-flow apparatus was filled with this membrane suspension while the other was filled with a similar solution without membranes and a different mannitol concentration in order to obtain an osmotic perturbation upon mixing. One-to-one mixing was accomplished by applying 4 atm pressure. The final protein concentration after mixing was always between 50 and 150 μg/ml. The stopped-flow apparatus was thermostated at 35°C, unless stated otherwise. Signals of 3 to 5 subsequent runs under identical conditions were summed by an Apple IIe computer and after correction for the signal change of an equal amount of runs with no osmotic perturbation the data were analyzed on a PDP11 computer using a nonlinear least-squares fitting program.

Electron Microscopy

To determine vesicular dimensions, electron micrographs were taken on a TEM-300 electron microscope. Pellets of membrane vesicles were fixed with 2% glutaraldehyde in a 0.1 M phosphate buffer, pH 7.4, washed with 0.1 M phosphate buffer (pH 7.4), treated with 1% OsO_4 and washed twice again with the same phosphate buffer. After dehydration and embedding in Epon, thin sections were stained with uranyl and lead citrate. Vesicular structures from randomly chosen micrographs were stereologically analyzed on a desk computer (Videoplan, Kontron GmbH FRG).

Theory

When volume changes of membrane vesicles are followed via changes in turbidity or light scattering one has to know the exact relationship between the optical signal and the vesicular volume. This problem has been approached experimentally [1, 34] and theoretically using the Mie and van de Hulst equations [23, 24]. However, Koch [21, 22] showed that the applicability of the more simple Rayleigh-Gans approximation can be extended to large particles such as mitochondria and bacteria for turbidity as well as light-scattering measurements.

Starting from the Rayleigh-Gans approximation the turbidity or light scattering can be written as

$$S = h \cdot F \cdot Q \tag{1}$$

in which h is independent of the vesicular properties and F and Q are functions described in detail by Chong and Colbow [5].

A simple way to relate the optical signal S to the change in vesicular radius R is to take the logarithmic form of Eq. (1) and differentiate it.

$$\frac{d \ln S}{d \ln R} = \frac{d \ln F}{d \ln R} + \frac{d \ln Q}{d \ln R}. \tag{2}$$

Now the relation between S and vesicular volume is

$$\frac{d \ln S}{d \ln V} = \frac{1}{3} \frac{d \ln S}{d \ln R} = -X. \tag{3}$$

It has been shown previously that F is fairly insensitive to changes in R [5].

When vesicles are mixed with a hypertonic solution with one impermeable solute the volume flow J_v is given by the equation

$$J_v = \frac{dV}{Adt} = -L_p RT \Delta C \simeq -\overline{V}_w P_f \Delta C \tag{4}$$

where $\frac{dV}{dt}$ is the volume change per unit time, A the membrane area, L_p the hydraulic conductivity, R and T the gas constant and temperature in °K, $\overline{V}_w$ the molar water volume, P_f the osmotic water permeability and ΔC the osmotic gradient in Osm/liter [20].

Combining Eqs. (3) and (4) results in

$$\frac{dS}{Sdt} = -X \frac{dV}{Vdt} = X \overline{V}_w P_f \frac{A}{V} \Delta C. \tag{5}$$

In Eq. (5) the magnitude of S is uncertain since leaky vesicles contribute to S but not to dS/dt. Also X is not exactly known.

Experimentally, vesicles with an initial vesicular volume V_o in an osmotic medium C_o, are mixed with a solution with osmolarity C_m. V_o will change to the end value V_∞. Since vesicles have an osmotically inactive volume b, the osmotic equation will be

$$C(V - b) = C_o(V_o - b) = C_m(V_\infty - b). \tag{6}$$

Assuming that P_f and A in Eq. (4) remain constant and using Eq. (6), then Eq. (4) can be integrated exactly with the result:

$$\ln \left\{ \frac{V_\infty - V}{V_\infty - V_o} \right\} - \frac{V - V_o}{V_\infty - V_o} \cdot \frac{\Delta C_o}{C_o} = -K \cdot t \tag{7a}$$

where $\Delta C_o = C_m - C_o$ and

$$K = \overline{V}_w P_f \frac{A}{V_o} \left(1 - \frac{b}{V_o}\right)^{-1} \frac{C_m^2}{C_o}. \tag{7b}$$

A similar result was obtained before by Macey [25] and Terwilliger and Solomon [35].

Equation (7a) can be approximated by a more simple equation realizing that $(V - V_o)/V_\infty - V_o)$ is relatively important in the initial stage of the process when the logarithmic term is still small. Therefore we can make the approximation:

$$\frac{V - V_o}{V_\infty - V_o} \simeq \left(\frac{dV}{\Delta V dt}\right)_o \cdot t = \overline{V}_w \cdot P_f \frac{A}{V_o} \left(1 - \frac{b}{V_o}\right)^{-1} C_m t \tag{8}$$

where $\Delta V = V_\infty - V_o$.

Substituting Eq. (8) into Eq. (7) we obtain

$$\ln\left\{\frac{V_\infty - V}{V_\infty - V_o}\right\} = -K_e t \tag{9a}$$

where

$$K_e = \bar{V}_w P_f \frac{A}{V_o}\left(1 - \frac{b}{V_o}\right)^{-1} C_m. \tag{9b}$$

This approximation yields a simple exponential function with a rate constant proportional to C_m. This result differs from the "small perturbation" theory of Farmer and Macey [8], which resulted in a simple exponential behavior with a rate constant proportional to C_m^2/C_o. The optical signal can now be introduced using Eq. (3). From $\frac{d \ln S}{d \ln V} = -X$ we obtain

$$V = H \cdot S^{-1/X} \tag{10}$$

where H results from integration.

Substituting Eq. (10) into Eq. (7) and making use of the approximation

$$(1 - a^{-1/X}) \simeq (1/X)(1 - a^{-1}) \tag{11}$$

we arrive at the following equation

$$\ln\left\{\frac{(S_\infty - S)}{(S_\infty - S_o)} \cdot \frac{S_o}{S}\right\} - \frac{(S - S_o)}{(S_\infty - S_o)} \cdot \frac{S_\infty}{S} \cdot \frac{\Delta C_o}{C_o} = -Kt \tag{12}$$

where K is defined as in Eq. (7b).

For the same reason as stated under (7a), Eq. (12) can be approximated by

$$\ln\left\{\frac{S_\infty - S}{S_\infty - S_o}\right\} = -K_e t. \tag{13}$$

Equation (13) will deviate seriously from Eq. (7), which is shown in Fig. 1 where the left-hand sides of Eqs. (12) and (13) are compared with the left-hand side of Eq. (7) as a function of the progress of the volume change.

Despite these large deviations when Eq. (13) is used, it is still justified to interpret the optical signal as a single exponential as long as the appropriate rate constant K_e is used as defined in Eq. (9b). Experimental evidence for this approach will be given in the Results section.

For calculation of P_f values we have fitted the optical signals to one- and to two-exponential functions:

$$S = S_\infty - \Delta S \exp(-K_e t) \tag{14}$$

and

$$S = S_\infty - \Delta S_s \exp(-K_s t) - \Delta S_f \exp(-K_f t) \tag{15}$$

where ΔS_s and ΔS_f correspond to the signal changes with either a slow rate constant K_s or a fast one K_f. K_e, K_s and K_f are interpreted as in Eq. (9b).

From $\Delta S = \Delta S_s + \Delta S_f$ a weighted averaged rate constant K_{de} can be determined

$$K_{de} = \left(\frac{dS}{\Delta S dt}\right)_o = \frac{K_s \Delta S_s + K_f \Delta S_f}{\Delta S}. \tag{16}$$

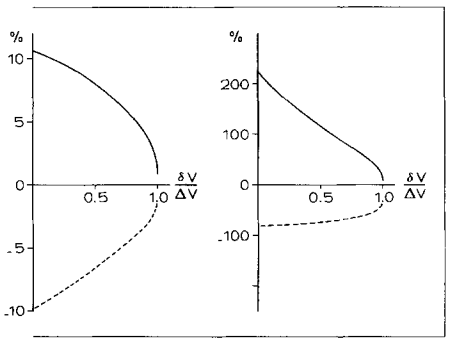

Fig. 1. Percentage deviation of the left-hand side of Eq. (12) (left panel) and Eq. (13) (right panel) from the left-hand side of Eq. (7a), as a function of the progress of the vesicular volume change ($\delta V/\Delta V$). $\Delta V = V_\infty - V_o$ and $\delta V = V - V_o$. For calculations the value $X = \frac{2}{3}$ (Eq. 3) has been used. Solid line: $C_o = 0.1$ Osm and $C_m = 0.3$ Osm; Dotted line: $C_o = 0.4$ Osm and $C_m = 0.1$ Osm

Results

Wavelength and Vesicular Volume Dependence of the Optical Signal

The turbidity τ for suspensions of intestinal and renal BBM vesicles was measured between 350 and 750 nm. The value $d \ln \tau / d \ln \lambda$ varied slightly with the aperture but was between -1.6 and -1.5. For 90° scattered light the value $d \ln S / d \ln \lambda$, had a minimum of -1.6. However, the sensitivity of the photomultiplier tube varied with the wavelength. In this study all experiments with scattered light were done at 400 nm. The volume dependence of 90° scattered light intensity could be estimated to be $d \ln S / d \ln V = -0.87$ (Eq. 3). Yoshikawa et al. [43] reported an X value of 0.67 for liposome suspensions, applying the Mie theory.

Osmotically Induced Changes in Scattered Light Intensity

In Fig. 2 a typical example is given of the time course of the scattered light intensity when renal and intestinal BBMV's are rapidly mixed with a hypertonic solution. There is a striking difference between the two BBMV populations. The scattered light from renal BBMV suspension increases much faster in intensity after osmotic perturbation. In Figs. 3 and 4 the changes in scattered light intensities from renal and intestinal BBMV suspensions have been fitted to a single and to a double-exponential function. It is obvious that with intestinal BBMV the fit is good with one exponential, which suggests a rather homogeneous vesicle population. With renal BBMV the fit to a double-exponential function is better than the fit to one exponential. This result

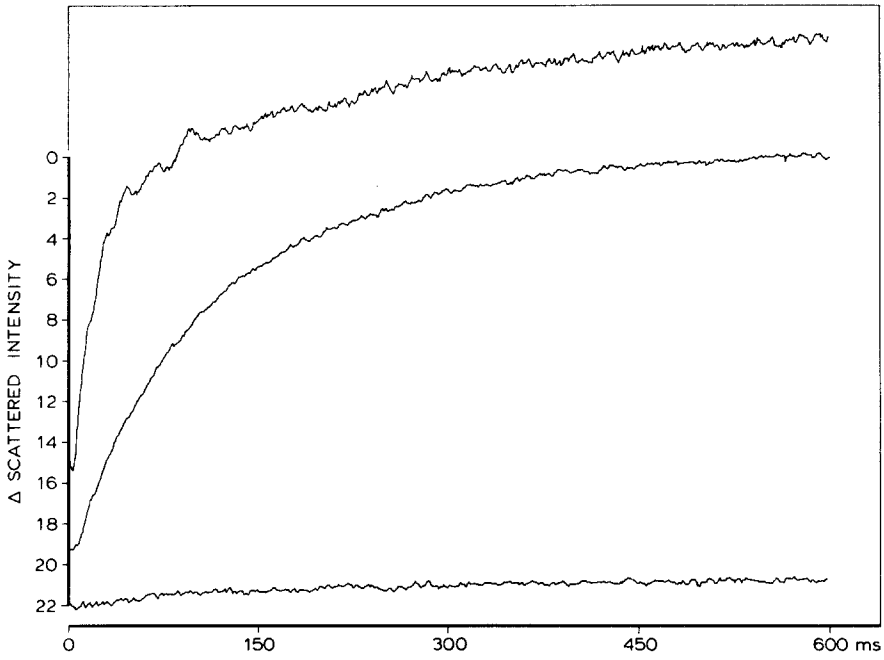

Fig. 2. Time course of change in scatter intensity after osmotic perturbation of rat renal and intestinal brush border vesicles. Upper curve: renal BBMV; middle curve: intestinal BBMV; lower curve: isoosmotic experiment (C_o = C_m = 116 mOsm). C_o = 116 mOsm; C_m = 219 mOsm. The traces represent a summation of five single shots

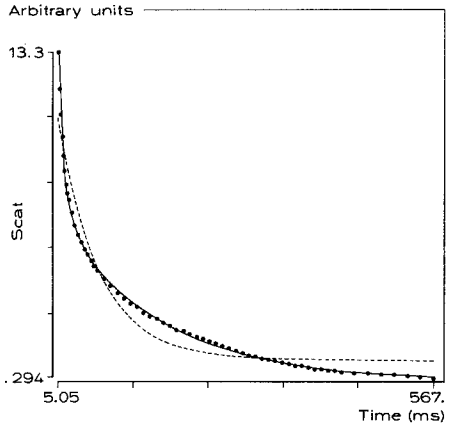

Fig. 3. Computer fit of change in scatter intensity from a renal brush border membrane preparation, after correction for the isotonic response. Solid line: double-exponential fit; Dotted line: single-exponential fit

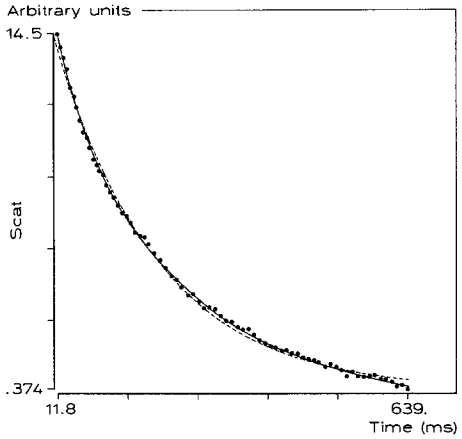

Fig. 4. Computer fit of change in scatter intensity from a small intestinal brush border membrane preparation, after correction for the isotonic response. Solid line: double-exponential fit; Dotted line: single-exponential fit

points to an inhomogeneity either in vesicle size or in water permeability.

Interpretation of Rate Constants

For calculating osmotic water permeability P_f, we have used the simplified exponential approximation as outlined under Theory (Eq. 13). To justify this approach we did osmotic shrinking experiments with rat intestinal BBMV and increasing osmotic gradients. The correct interpretation of the rate constant K was obtained from plots of the left-hand side of Eq. (12) versus t in which K is interpreted as in Eq. (7b). The single-exponential approach gives us the rate constant K_e. In Fig. 5 the osmotically corrected rate constants are plotted as a function of the medium osmolarity. It is obvious that within each single experiment there is a much better agreement between K_e/C_m and the correct interpretation $K \cdot C_o/C_m^2$ than between $K_e \cdot C_o/C_m^2$ and $K \cdot C_o/C_m^2$. The last interpretation, $K_e \cdot C_o/C_m^2$, used by Macey's group [8, 25] obviously leads to the erroneous conclusion that water permeability is a function of osmolarity. When the rate constants $K \cdot C_o/C_m^2$

Table 1. Osmotically corrected rate constants sec^{-1} Osm^{-1} for rat renal and intestinal plasma membrane vesicles, and the dimensional parameters

	Intestine		Kidney	
	BBM (n = 4)	BLM (n = 3)	BBM (n = 9)	BLM (n = 4)
K_e/C_m[a]	34.0 ± 0.2	29 ± 8	130 ± 19	41 ± 10
K_{de}/C_m[b]	43.7 ± 0.3	44 ± 11	263 ± 7	68 ± 19
K_s/C_m[c]	—	—	37 ± 3	23 ± 12
K_f/C_m[d]	—	—	443 ± 15	130 ± 32
V_o/A	35 nm	35 nm	35 nm	90 nm
$(1 - b/V_o)$[e]	0.72	0.72	0.72	0.88

[a] K_e, rate constant from a single-exponential fit (Eq. 14).
[b] K_{de}, weighted averaged rate constant from a double-exponential fit (Eq. 16).
[c,d] K_s, K_f, slow and fast rate constant of a double-exponential fit (Eq. 15).
[e] b = osmotic inactive vesicle volume calculated from $(R - 10)^3/R^3$, assuming a membrane thickness of 10 nm.

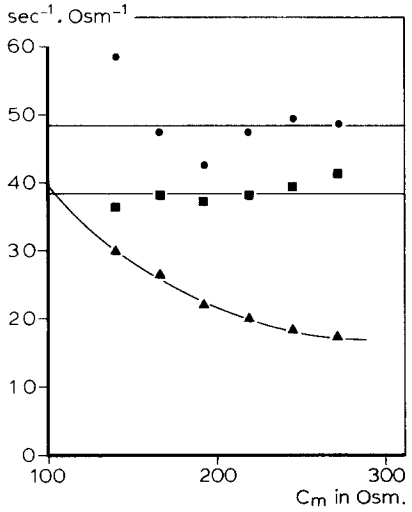

Fig. 5. Comparison of osmotically corrected rate constants (S^{-1} · Osm^{-1}) from osmotic shrinking experiments with intestinal brush borders. ●—● $K \cdot C_o/C_m^2$ according to Eqs. (12) and (7b); ■—■ K_e/C_m according to Eqs. (13) and (9b); ▲—▲ $K_e \cdot C_o/C_m^2$ according to Eqs. (12) and (7b); C_o = 0.116 osm

and K_e/C_m are used the water permeability turns out to be independent of the medium osmolarity.

In all further experiments we have used the simple exponential approximation and interpreted the rate constant K_e as in Eq. (9b).

Vesicular Dimensions

The dimensions of the vesicles of renal and intestinal BBM and BLM were determined from electron micrographs of thin sections. The BBM vesicles were of uniform size and an average value for V_o/A could easily be obtained. The BLM vesicles were less uniform. The renal BLM preparation especially contained larger vesicles with more irregular shapes. In Fig. 6 the histograms are given for the dimensions of the four membranes used. All, except the renal BLM have calculated V_o/A ratios of about 35 nm. This ratio varied between 40 to 90 nm for renal BLMV's.

Table 2. Osmotic water permeabilities of rat renal and intestinal brush border and basolateral membrane vesicles

	P_f (μm/sec)	
	BBM	BLM
Small intestine	60 ± 0.4* (4)[a]	60 ± 15* (3)
Kidney	359 ± 10* (9)	291 ± 81* (4)
Fast component	604 ± 20 (58%)	557 ± 137 (46%)
Slow component	50 ± 4 (42%)	99 ± 5 (54%)

* Calculated from the weighted rate constant K_{de} of a double-exponential fit.
[a] Mean values ± SE with number of experiments in parentheses. In case of two exponentials the percentage in parentheses means:

$$\frac{\Delta S_f}{\Delta S} \times 100\% \quad \text{or} \quad \frac{\Delta S_s}{\Delta S} \times 100\%.$$

Osmotic Water Permeabilities

All data were fitted to a single- and to a double-exponential function. In Table 1 the dimensional parameters and the rate constants are summarized which have been used for calculating the osmotic water permeabilities of the four membrane types. Table 2 gives the calculated P_f values for renal and intestinal membranes. The P_f values for renal mem-

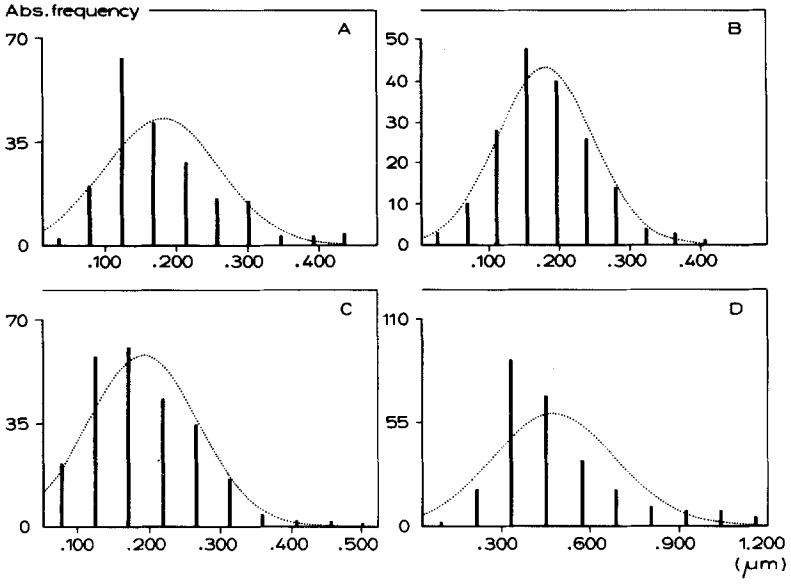

Fig. 6. Histograms of vesicular diameters calculated from stereological analyses of electron micrographs. (*A*) Rat intestinal brush border membranes; (*B*) Rat intestinal basolateral membranes; (*C*) Rat renal brush border membranes; (*D*) Rat renal basolateral membranes. The dotted lines indicate the gaussian distributions around the mean values with standard deviations. Mean values ± SE for diameters are: (*A*) 0.180 ± 0.081 μm, n = 197; (*B*) 0.181 ± 0.068 μm, n = 177; (*C*) 0.191 ± 0.078 μm, n = 243; (*D*) 0.474 ± 0.207 μm, n = 265

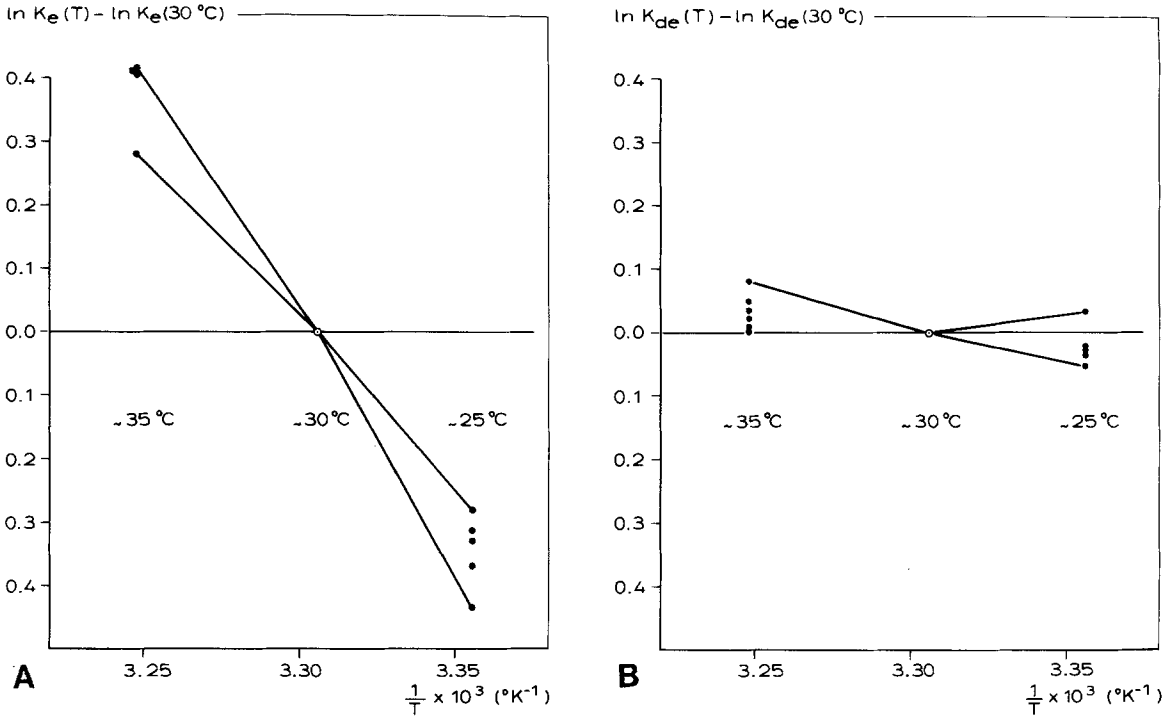

Fig. 7. Temperature dependence of osmotic shrinking behavior of brush border membranes. (*A*) Rat small intestine; K_e obtained from single exponential fit. (*B*) Rat renal cortex weighted averaged K_{de} from double-exponential fit. All experiments were done with C_o = 0.116 mOsm and C_m = 0.219 mOsm

branes are significantly higher than those for small intestine. This difference becomes even more striking when the fast and slow components of the optical signal are used separately in calculating P_f values. Roughly half of the renal vesicles have a 10-fold higher P_f value than the intestinal vesicles. The other half has similar P_f values as the intestine. Another important observation is that both cell

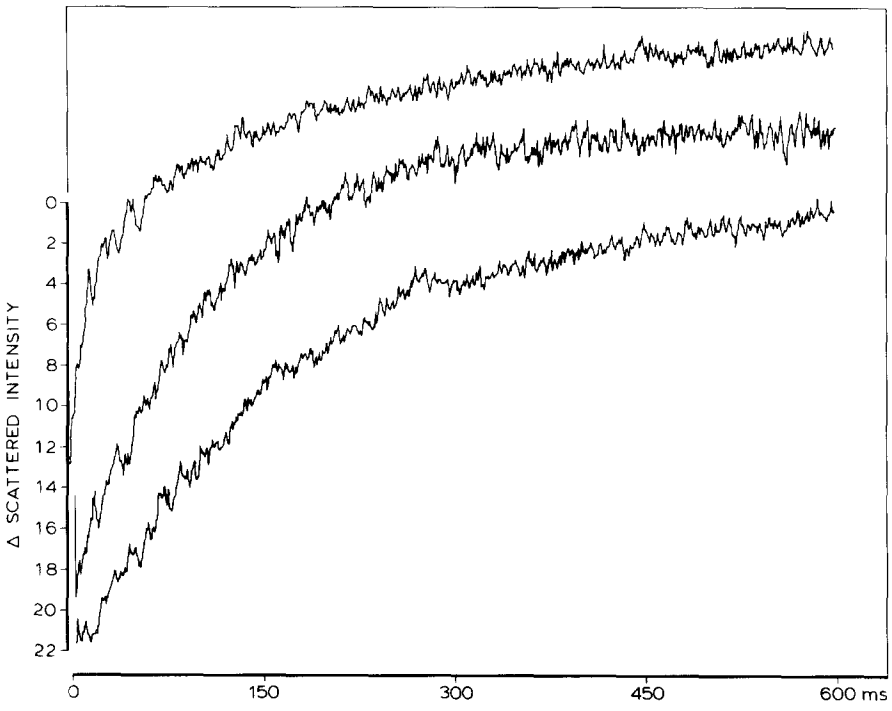

Fig. 8. Effect of *p*CMBS on change in scattered light intensity from rat renal brush border membranes. Upper curve: untreated control; Middle curve: after 45-min exposure to 1.5 mM *p*CMBS; Lower curve: after 5-min exposure to 10 mM *p*CMBS

poles have equal water permeabilities which suggests that cortical renal and small intestinal cells are symmetrical with respect to water flows.

Apparent Activation Energies and Effect of *p*CMBS

Since P_f values of renal membranes are one order of magnitude larger than those for intestine we studied the temperature dependence. Osmotic shrinking experiments were done at 25, 30 and 35°C with five intestinal and six renal brush border preparations. The results are shown in Figs. 7*A* and *B*. The slopes of the Arrhenius plots yields a mean value for the apparent activation energy of 13.3 ± 0.6 kCal/mol for intestinal BBMV, with a minimum value of 9.6 kCal/mol. For renal BBMV there was almost no influence of temperature on P_f between 25 and 35°C. The mean value for activation energy was 1.0 ± 0.3 kCal/mol. The low activation energy for the renal water permeability suggests that water can cross the membrane relatively free, possibly through water channels. Water permeation through intestinal membranes is most likely through the lipid matrix.

Water permeability mediated by water channels has been shown to be reversibly inhibited by mercurial sulfhydryl reagents such as *p*CMBS (*p*-chloromercuribenzene sulfonate) [26]. For this reason we studied the effect of *p*CMBS on renal BBMV water permeability. In Fig. 8 the effect of *p*CMBS on osmotic shrinking of renal BBMV is shown. With 10 mM *p*CMBS the fast component of the shrinking process completely disappeared after 5-min exposure to the drug. At 1.5 mM the inhibition process can be followed more closely since it takes 30 min before the inhibition is completed. In Table 3 a typical example is given of the time course of the inhibition of water permeability by *p*CMBS.

Three conclusions can be drawn from Table 3: i) the contribution of the fast component to the total change in scatter intensity (ΔS_f as % of ΔS) is reduced by *p*CMBS, but the high P_f value is relatively unaffected by *p*CMBS. This result is most easily interpreted if water channel closure is all or none. Apparently, *p*CMBS acts by reducing the number of channels. A similar conclusion was reached for red blood cell water channels by Macey [26]; ii) *p*CMBS acts reversibly on renal water channels since dithiothreitol restores the contribution of the fast component to the scatter signal; iii) The low P_f value, most likely the lipid matrix permeability, increases by *p*CMBS.

The experiments shown in Fig. 8 and Table 3 were repeated with two other membrane preparations with similar results. In addition, *p*CMBS had no effect on osmotic shrinking of small intestinal BBMV.

Table 3. *p*CMBS effect on osmotic water permeability of rat renal brush border membrane vesicles

	Change in scatter intensity (% of ΔS)		P_f (μm/sec)	
	Fast (ΔS_f)	Slow (ΔS_s)	High	Low
Control	47	53	450	37
p CMBS exposure time: 5 min	45	55	444	66
10	51	49	480	75
15	43	57	333	92
20	38	62	330	72
30	8	92	329	76
60-min *p*CMBS[a] + 25-min DTT[b]	36	64	380	87

[a] *p*CMBS, *p*-chloromercuribenzene sulfonate (1.5 mM).
[b] DTT, dithiothreitol (1.5 mM).

Discussion

Methodological Aspects

Changes in scattered light intensity were used to follow the osmotic shrinking of renal and intestinal membrane vesicles and from these experiments osmotic water permeabilities were calculated. Although the principle has been widely used for erythrocytes, membrane vesicles and liposomes, most studies use this method for comparing solute permeabilities and not to extract absolute values for permeabilities [1, 19, 25, 32]. We justified our approach both theoretically and experimentally and concluded that a simple exponential approximation can be used provided the rate constant K_e is considered being proportional to C_m and not to C_m^2/C_o, and as long as $d \ln S/d \ln V$ does not deviate too much from -1 (Figs. 1,5).

The size analysis based on electronmicroscopy (Fig. 6) showed a gaussian distribution around a mean value for all four preparations, suggesting a reasonably homogeneous vesicle preparation with respect to size. In a recent study it was demonstrated that size analysis of membrane vesicles by means of electronmicroscopy, gel filtration and quasi elastic light scattering yielded identical dimensional parameters [29]. Moreover, the size for BBM vesicles reported by Perevucnik et al. [29] is identical to our values in Fig. 6*A*,*C*. In our study only renal BLM vesicles were significantly larger, which could be due to the mild homogenization step with a Dounce apparatus [15]. Also canine renal BLMV were irregularly shaped with vesicle diameters ranging between 0.5 and 1.0 μm [41].

Although the size distribution is rather homogeneous, the degree of resealing may present a problem in interpreting permeability coefficients of membrane vesicles. It is obvious that vesicles with a $\sigma \simeq o$ for mannitol do not contribute to osmotic shrinking. These vesicles contribute to the scatter intensity S_o but not to ΔS after osmotic perturbation. Therefore the value $\frac{\Delta S}{S_o} \cdot \frac{C_m}{\Delta C_o}$ provides information about the percentage of osmotically active vesicles. This value was twice as high for BBM as for BLM preparations, suggesting twice as many resealed vesicles in BBMV than in BLMV counterparts. The agreement with previous data is striking, since BLM preparations of small intestine and renal cortex contain 40 to 50% leaky vesicles, based on latency in Na^+,K^+-ATPase activity [11, 15]. In another study we estimated mannitol and salt permeability coefficients of renal and intestinal BBMV and found values around 1 nm/sec which is 5 orders of magnitude smaller than P_f values for these membranes [17]. We also observed that after storage of vesicles in liquid N_2 the solute permeability increased twofold while the water permeability remained unchanged (*unpublished observation*). It is therefore unlikely that small differences in mannitol permeabilities among membrane vesicles will affect P_f measurements seriously.

Brush border and basolateral membrane preparations are contaminated with membranes derived from intracellular organelles. How does this affect the conclusions of our study? The optical signal from intestinal BBMV and BLMV fit well with one exponential function. This implies a homogeneity in size and in water permeability of the membranes present in these preparations. Therefore, intracellular membranes either have the same P_f value as plasma membranes or do not contribute to ΔS because they are too leaky. The first possibility is most likely and could also explain the two P_f values found for renal BBM and BLM preparations. The high P_f value reflects the plasma membranes and the

Table 4. Osmotic water permeabilities of epithelial cell membranes[a]

	P_f (μm/sec)		Preparation	Source
	Brush border	Basolateral		
Rat kidney cortex	604	557	Vesicles	This study
Rabbit kidney cortex	110	—	Vesicles	Verkman et al. [36]
Rabbit kidney PCT	—	293	Intact cells	Welling et al. [39]
PST	—	345	Intact cells	Welling et al. [39]
PST	—	340	Intact cells	Capri-Medina et al. [4]
Rat small intestine	60	60	Vesicles	This study
	12 (25°C)	—	Vesicles	Worman & Field [42]
Necturus gallbladder	70[b]	50[b]	Intact cells	Persson & Spring [30]
Corneal endothelium	300–600	—	Intact cells	Fishbarg [10]

[a] All data per unit membrane area.
[b] Per unit membrane area as cited in Berry [2].

low P_f value the intracellular membranes. Since both contributions to ΔS are roughly equal (Table 2) this means that about 50% of the membranes could be of plasmalemmal origin. This possibility is supported by recent work on Na^+/H^+ exchange in renal BBM. Mircheff et al. [27] demonstrated that conventional renal BBM preparations can be resolved into four distinct membrane populations with a counter-current distribution technique. Roughly 50% of the membranes were of plasmalemmal origin, an estimate in good agreement with our interpretation of the two components of ΔS.

Physiological Meaning of P_f Values of Membrane Vesicles

Osmotic permeabilities obtained in this study are compared with recent P_f values from the literature in Table 4. When differences in techniques and species are taken into consideration, it is surprising that our P_f values for renal membranes are almost equal to those reported by Welling et al. [39] and Carpi-Medina et al. [4] measured on intact proximal tubular cells. Our P_f values for intestinal membranes are similar to Persson and Spring's [30] values for intact gallbladder cells. Recently Verkman et al. [36] reported a fivefold lower P_f for rabbit renal BBMV. In the initial stage of our study we used rabbit renal BBMV and found a similar low P_f value [16]. Moreover, we never found two different vesicle populations as in rat renal cortex. At the moment this species difference is puzzling but deserves further study. It is feasible that either cytoskeletal elements in rabbit BBMV affects the osmotic response or that water channels become inactivated or partly damaged during membrane isolation. Worman and Field's [42] P_f value for rat intestinal BBMV is small compared to our value but these authors worked at 25°C, did not correct for the osmotic inactive space and used Macey's small perturbation theory. All three factors work in the same direction, i.e., underestimation of the P_f value.

An important conclusion from our study is that BBM and BLM have equal P_f values. In rabbit proximal tubules, Welling and Welling [37] showed that the brush border area and the lateral cell wall area are equal. Hence, proximal tubular cells are symmetrical with respect to water permeability. The same conclusion was reached for gallbladder epithelium [30]. Combining Welling's estimate [37, 38] for membrane area amplification (46 cm^2/cm^2 epithelial surface) and our P_f values, then the transcellular P_f value can be calculated and amounts to 1.38 cm/sec. Measured transepithelial P_f values range between 0.2 and 0.7 cm/sec [2]. Therefore, an entirely transcellular route for water flow is a realistic possibility and the paracellular pathway may be rather insignificant. This conclusion was also reached by Preissig and Berry [31] based on calculations using realistic dimensions for the shunt pathway.

With a transepithelial P_f value around 1 cm/sec, the transcellular osmotic gradient needed to drive volume absorption, with a rate of 2 to 4 nl/min · mm tubular length, can be calculated to be 2.5 to 5 mOsm (*see also* [2]). The small luminal hypotonicity recently demonstrated in rat proximal tubules falls within this range [12]. These calculations demonstrate that P_f values of membrane vesicles, as obtained in our study, are in line with the hypothesis that luminal hypotonicity drives fluid absorption in proximal tubules [33].

The high activation energy for water permeability of intestinal brush borders strongly suggests a lipid solubility-diffusion mechanism for water per-

meation [9]. For renal membranes the possibility of water channels as an alternative is very likely. Firstly, the low activation energy for water permeation is compatible with those found for red blood cells of various species [26], ADH-treated toad bladder [7] and cortical collecting tubules [14]. Secondly, in renal membranes *p*CMBS inhibits water permeability in an all-or-none mode as described in red blood cells [26]. Whittembury et al. [40] also demonstrated an effect of *p*CMBS on water permeability of lateral membranes in intact proximal tubules. The likelihood of water channels in renal cortical membranes makes a more biochemical approach to characterize these channels feasible, since large amounts are readily available from slaughterhouse material.

Our final conclusion is that osmotic studies on isolated membrane vesicles provide realistic values for the osmotic water permeability of epithelial cells. The renal plasma membranes are one order of magnitude more permeable for water than the intestinal counterpart and most likely water channels are responsible for the high P_f value in renal membranes.

Electron microscopy was performed by Dr. W. Eling, Department of Cytohistology. The stereology counting device was made available by Dr. G. Eggberink, Department of Electronmicroscopy. The final version of the manuscript was typed by Mrs. S. Engels. This study was in part supported by the Netherlands Organization for the Advancement of Basic Research (ZWO) through the Foundation of Biophysics (12-25-16).

References

1. Bangham, A.D., De Gier, J., Greville, G.D. 1967. Osmotic properties and water permeability of phospholipid liquid crystals. *Chem. Phys. Lipids* **1**:225–246
2. Berry, C.A. 1983. Water permeability and pathways in the proximal tubule. *Am. J. Physiol.* **245**:F279–F294
3. Biber, J., Stieger, B., Haase, W., Murer, H. 1981. A high yield preparation for rat kidney brush-border membranes. *Biochim. Biophys. Acta* **647**:169–176
4. Carpi-Medina, P., Lindemann, B., González, E., Whittembury, G. 1984. The continuous measurement of tubular volume changes in response to step changes in contraluminal osmolality. *Pfluegers Arch.* **400**:343–348
5. Chong, C.S., Colbow, K. 1976. Light scattering and turbidity measurements on lipid vesicles. *Biochim. Biophys. Acta* **436**:260–282
6. Diamond, J.M. 1979. Osmotic water flow in leaky epithelia. *J. Membrane Biol.* **51**:195–216
7. Eggena, P. 1972. Temperature dependence of vasopressin action on the toad bladder. *J. Gen. Physiol.* **59**:519–533
8. Farmer, R.E.L., Macey, R.I. 1970. Perturbation of red cell volume: Rectification of osmotic flow. *Biochim. Biophys. Acta* **196**:53–65
9. Fettiplace, R., Haydon, D.A. 1980. Water permeability of lipid membranes. *Physiol. Rev.* **60**:510–550
10. Fishbarg, J. 1982. The paracellular pathway in the corneal endothelium. *In:* The Paracellular Pathway. S.E. Bradley and E.F. Purcell, editors. pp. 307–318. Macey Foundation, New York
11. Ghijsen, W.E.J.M., Jong, M.D. de, Os, C.H. van 1982. ATP-dependent calcium transport and its correlation with Ca^{2+}-ATPase activity in basolateral membranes of rat duodenum. *Biochim. Biophys. Acta* **689**:327–336
12. Green, R., Giebisch, G. 1984. Luminal hypotonicity: A driving force for fluid absorption from the proximal tubule. *Am. J. Physiol.* **246**:F167–F174
13. Hauser, H., Howell, K., Dawson, R.M.C., Bowyer, D.E. 1980. Rabbit small intestine brush border membrane preparation and lipid composition. *Biochim. Biophys. Acta* **602**:567–577
14. Hebert, S.C., Andreoli, T.E. 1982. Water movement across the mammalian cortical collecting duct. *Kidney Int.* **22**:526–535
15. Heeswijk, M.P.E. van, Geertsen, J.A.M., Os, C.H. van 1984. Kinetic properties of the ATP-dependent Ca^{2+} pump and the Na^+/Ca^{2+} exchange system in basolateral membranes from rat kidney cortex. *J. Membrane Biol.* **79**: 19–31
16. Heeswijk, M.P.E. van, Os, C.H. van 1984. Hydraulic conductivity of rabbit kidney brush-border membrane vesicles. *J. Physiol. (London)* **348**:27P
17. Heeswijk, M.P.E. van, Os, C.H. van 1986. Water and salt permeabilities of brush border membrane vesicles from rat small intestine and kidney cortex. *In:* Ion Gradient-Coupled Transport. A.F. Alvarado and C.H. van Os, editors. pp. 329–332. Elsevier, Amsterdam
18. Hill, A. 1980. Salt-water coupling in leaky epithelia. *J. Membrane Biol.* **56**:177–182
19. Kasai, M., Kanemasa, T., Fukumoto, S. 1979. Determination of reflection coefficients for various ions and neutral molecules in sarcoplasmic reticulum vesicles through osmotic volume change studied by stopped flow technique. *J. Membrane Biol.* **51**:311–324
20. Kedem, O., Katchalsky, A. 1958. Thermodynamic analysis of the permeability of biological membranes to non-electrolytes. *Biochim. Biophys. Acta* **27**:229–246
21. Koch, A.L. 1961. Some calculations on the turbidity of mitochondria and bacteria. *Biochim. Biophys. Acta* **51**:429–441
22. Koch, A.L. 1968. Theory of the angular-dependence of light scattered by bacteria and similar-sized biological objects. *J. Theor. Biol.* **18**:133–156
23. Latimer, P., Moore, D.M., Bryant, F.D. 1968. Changes in total light scattering and absorption caused by changes in particle conformation. *J. Theor. Biol.* **21**:348–367
24. Latimer, P. 1983. Photometric assay of cell shrinkage. *J. Theor. Biol.* **102**:249–259
25. Macey, R.I. 1979. Transport of water and non-electrolytes across red cell membranes. *In:* Membrane Transport in Biology. G. Giebisch, D.C. Tosteson, and H.H. Ussing, editors. pp. 1–54. Springer, Berlin
26. Macey, R.I. 1984. Transport of water and urea in red blood cells. *Am. J. Physiol.* **246**:C195–C203
27. Mircheff, A.K., Ives, H.E., Yee, V.J., Warnock, D.G. 1984. Na^+/H^+ antiporter in membrane populations resolved from a renal brush border vesicle population. *Am. J. Physiol.* **246**:F853–F858
28. Mlekoday, J.H., Moore, R., Levitt, D.G. 1983. Osmotic water permeability of the human red cell. *J. Gen. Physiol.* **81**:213–220

29. Perevucnik, G., Schurtenberger, P., Lasic, D.D., Hauser, H. 1985. Size analysis of biological membrane vesicles by gel filtration, dynamic light scattering and electron microscopy. *Biochim. Biophys. Acta* **821:**169–173
30. Persson, E., Spring, K.R. 1982. Gallbladder epithelial cell hydraulic permeability and volume regulation. *J. Gen. Physiol.* **79:**481–505
31. Preissig, P.A., Berry, C.A. 1985. Evidence for transcellular osmotic water flow in rat proximal tubules. *Am. J. Physiol.* **249:**F124–F131
32. Rabon, E., Takeguchi, N., Sachs, G. 1980. Water and salt permeability of gastric vesicles. *J. Membrane Biol.* **53:**109–117
33. Schafer, J.A. 1984. Mechanisms coupling the absorption of solutes and water in the proximal nephron. *Kidney Int.***25:**708–716
34. Tedeschi, H., Harris, D.L. 1958. Some observations on the photometric estimation of mitochondrial volume. *Biochim. Biophys. Acta* **28:**392–402
35. Terwilliger, T.C., Solomon, A.K. 1981. Osmotic water permeability of humen red cells. *J. Gen. Physiol.* **77:**549–570
36. Verkman, A.S., Dix, J.A., Seifter, J.L. 1985. Water and urea transport in renal microvillus membrane vesicles. *Am. J. Physiol.* **248:**F650–F655
37. Welling, L.W., Welling, D.J. 1975. Surface areas of brush border and lateral cell walls in the rabbit proximal nephron. *Kidney Int.* **8:**343–348
38. Welling, L.W., Welling, D.J. 1976. Shape of epithelial cells and intercellular channels in the rabbit proximal nephron. *Kidney Int.* **9:**385–394
39. Welling, L.W., Welling, D.J., Ochs, T.J. 1983. Video measurements of basolateral membrane hydraulic conductivity in the proximal tubule. *Am. J. Physiol.* **245:**F123–F129
40. Whittembury, G., Paz-Aliaga, A., Biondi, A., Carpi-Medina, P., Gonzalez, E., Linares, H. 1985. Pathways for volume flow and volume regulation in leaky epithelia. *Pfluegers Arch.* **405:**S17–S22
41. Windus, D., Cohn, D., Klahr, S., Hammerman, M.R. 1984. Glutamine transport in renal basolateral vesicles from dogs with metabolic acidosis. *Am. J. Physiol.* **246:**F78–F86
42. Worman, H.J., Field, M. 1985. Osmotic water permeability of small intestinal brush-border membranes. *J. Membrane Biol.* **87:**233–239
43. Yoshikawa, W., Akutsu, H., Kyogoku, Y. 1983. Light-scattering properties of osmotically active liposomes. *Biochim. Biophys. Acta* **735:**397–406

Received 23 January 1986; revised 3 March 1986